



Title	Redox regulation in radiation-induced cytochrome c release from mitochondria of human lung carcinoma A549 cells.
Author(s)	Ogura, Aki; Oowada, Shigeru; Kon, Yasuhiro; Hirayama, Aki; Yasui, Hironobu; Meike, Syunsuke; Kobayashi, Saori; Kuwabara, Mikinori; Inanami, Osamu
Citation	Cancer Letters, 277(1), 64-71 <a href="https://doi.org/10.1016/j.canlet.2008.11.021">https://doi.org/10.1016/j.canlet.2008.11.021</a>
Issue Date	2009-05-08
Doc URL	<a href="http://hdl.handle.net/2115/38355">http://hdl.handle.net/2115/38355</a>
Type	article (author version)
File Information	Cancer_Letters.pdf



[Instructions for use](#)

**REDOX REGULATION IN RADIATION-INDUCED CYTOCHROME-C  
RELEASE FROM MITOCHONDRIA OF HUMAN LUNG CARCINOMA A549  
CELLS**

Aki Ogura<sup>1</sup>, Shigeru Oowada<sup>2</sup>, Yasuhiro Kon<sup>3</sup>, Aki Hirayama<sup>4</sup>, Hironobu Yasui<sup>1</sup>,  
Syunsuke Meike<sup>1</sup>, Saori Kobayashi<sup>5</sup>, Mikinori Kuwabara<sup>1</sup> and Osamu Inanami<sup>1\*</sup>

<sup>1</sup> Laboratory of Radiation Biology and <sup>3</sup> Laboratory of Anatomy, Graduate School of  
Veterinary Medicine, Hokkaido University, Kita 18 Nishi 9, Sapporo 060-0818, Japan;

<sup>2</sup> Department of Microbiology, St.Marianna University School of Medicine, 2-16-1  
Sugao, Miyamae-ku, Kawasaki 216-8511, Japan; <sup>4</sup> Center of Integrative Medicine,  
Tsukuba University of Technology, Ibaraki 305-8575, Japan; <sup>5</sup> Department of Veterinary  
Clinical Science, The United Graduate School of Veterinary Sciences, Gifu University,  
1-1 Yanagido, Gifu 501-1193, Japan

\*Corresponding author:

Tel: +81-11-706-5235

Fax: +81-11-706-7373

E-mail address: [inanami@vetmed.hokudai.ac.jp](mailto:inanami@vetmed.hokudai.ac.jp)

## Abstract

Mitochondria in mammalian cells were well-known to play an important role in the intrinsic pathway of genotoxic-agent-induced apoptosis by releasing cytochrome *c* into cytosol and to be a major source of reactive oxygen species (ROS). The aim of this study is to examine whether mitochondrial ROS involved in radiation-induced apoptotic signaling in A549 cells. The post-irradiation-treatment of N-acetyl-L-cystein (NAC) inhibited cytochrome *c* release from mitochondria but did not affect expression level of Bcl-2, Bcl-X<sub>L</sub> and Bax, suggesting late production of ROS triggered cytochrome *c* release. The experiments using DCFDA (a classical ROS fluorescence probe) and MitoAR (a novel mitochondrial ROS probe) demonstrated that intracellular and mitochondrial ROS were enhanced 6 h after X irradiation. Furthermore, the O<sub>2</sub><sup>-</sup> production ability of mitochondria isolated from A549 cells was evaluated by ESR spectroscopy combined with a spin-trapping reagent (CYPMPO). When isolated mitochondria were incubated with NADH, succinate and CYPMPO, the ESR spectrum due to CYPMPO-OOH was detected. This NADH/succinate-dependent O<sub>2</sub><sup>-</sup> production from mitochondria of irradiated cells was significantly increased in comparison with that of unirradiated cells. These results indicated that ionizing radiation enhanced O<sub>2</sub><sup>-</sup> production from mitochondria to trigger cytochrome *c* release in A549 cells.

Keywords: Radiation; Reactive oxygen species (ROS); Redox regulation; Mitochondria; Electron spin resonance (ESR)

## 1. Introduction

Mitochondria in mammalian cells are well-known to play an important role in the intrinsic pathway of genotoxic-agent-induced apoptosis by releasing proapoptotic proteins (i.e., cytochrome *c* [1] and Smac/DIABLO [2]) into cytosol. In hematopoietic cells, ionizing radiation easily leads to the cytochrome *c* release from mitochondria and cytosolic cytochrome *c* initiates the activation of downstream caspases and leads to apoptosis [3,4]. In our previous study in mouse fibroblast NIH3T3, human lung carcinoma A549 and human cervical carcinoma HeLa cells [5], the downstream signaling from this cytochrome *c* release was strongly inhibited by constitutive Survivin, a member of the inhibitor of apoptosis protein (IAP) family. However, transduction of adenoviral vectors for dominant negative mutants (pAd-T34A and pAd-D53A) was found to abrogate the function of constitutive Survivin and facilitate radiation-induced apoptotic cell death in tumor cells, indicating that Survivin is an ideal target for radiosensitization in solid tumor cells. Thus, the cytochrome *c* release from mitochondria is an essential event in radiation-induced apoptosis even in solid tumor cells, although this mechanism is still unclear.

Ionizing radiation is known to generate reactive oxygen species (ROS), i.e., OH radicals, H atoms and H<sub>2</sub>O<sub>2</sub>, through radiolysis of water [6,7]. In irradiated tissues and cells, the primary biological damage caused by the reaction of ROS with biomacromolecules (DNA, proteins, lipids, etc.) is believed to be produced within  $\sim 10^{-9}$  seconds and leads to serious biological consequences, i.e., cell death, cell cycle arrest, mutation and carcinogenesis [6-9]. Recently, we have demonstrated that radiation-induced apoptosis in human leukemia Molt-4 cells is remarkably inhibited if antioxidants such as N-acetyl-L-cystein (NAC) [10,11] and Trolox [12] are added to the

medium within several minutes after X irradiation. This suggests that the secondary production of ROS occurs as a late event after irradiation and that these secondary ROS play an important role in radiation-induced apoptotic signaling. In fact, Chen *et al.* report that intracellular ROS, detected by 2',7'-dichlorofluorescein diacetate (DCFDA) and dihydroethidium (DHE), gradually increased in multiple myeloma IM-7 and RPMI8226 cells after  $\gamma$  irradiation [13]. As a source of late intracellular ROS, the respiratory chain in mitochondria has been proposed in tumor cells exposed to genotoxic stimuli [14,15]. However, there is no direct evidence for a radiation-induced late increase of intracellular ROS derived from mitochondria because the sensitivity and specificity of fluorescence probes and spin-trapping reagents to detect ROS are insufficient.

In the present study, we investigated whether mitochondrial ROS were increased by X irradiation in solid tumor cells and involved in radiation-induced apoptotic signaling, especially cytochrome *c* release. To detect mitochondrial ROS, we used MitoAR, a novel mitochondria-derived ROS indicator [16]. Furthermore, the NADH/succinate-dependent  $O_2^{\cdot-}$  production ability of mitochondria isolated from A549 cells was also elucidated by electron spin resonance (ESR) spectroscopy with the spin-trapping technique. In this experiment, we employed 5-(2,2-dimethyl-1,3-propoxy cyclophosphoryl)-5-methyl-1-pyrroline N-oxide (CYPMPO), which was recently synthesized for the detection of  $O_2^{\cdot-}$  and OH radicals as the spin-trapping reagent [17].

## **2. Materials and methods**

### *2.1. Reagents*

5-(2,2-Dimethyl-1,3-propoxy cyclophosphoryl)-5- methyl-1-pyrroline N-oxide

(CYPMPO) was from Radical Research Inc. (Tokyo, Japan). Propidium iodide (PI), 2',7'-dichlorofluorescein diacetate (DCFDA) and diphenylene iodonium (DPI) were obtained from Sigma Chemical Company (St. Louis, MO). 6-Hydroxy-2,5,7,8-tetramethylchroman-2-carboxylic acid (Trolox) was from Calbiochem-Novabiochem International Inc. (San Diego, CA). N-tert-butyl- $\alpha$ -(2-sulfophenyl)-nitron (S-PBN) was purchased from Aldrich Chemical Co. (Milwaukee, WI). The following antibodies were used for western blotting: anti-actin and anti-Bax (Santa Cruz Biotechnology, Santa Cruz, CA), anti-Bcl-2 and anti-Bcl-X<sub>L</sub> (Wako, Osaka, Japan) and anti-cytochrome *c* (BD PharMingen, Erebodegem, Belgium). N-acetyl-L-cystein (NAC) and other reagents were obtained from Wako Pure Chemical Co. (Tokyo, Japan).

## *2.2. Cell culture, X irradiation and drug treatment*

Human lung carcinoma A549 cells were maintained in RPMI 1640 medium containing 10% fetal calf serum at 37°C in 5% CO<sub>2</sub>. X irradiation was performed with an X ray generator (1.0-mm aluminum filter, 200 kVp, 20 mA, Shimazu HF-350, Kyoto). The dose rate was 3.9 Gy/min, which was determined using Fricke's chemical dosimeter. NAC, Trolox, S-PBN and DPI were added to the growth medium immediately after X irradiation and cells were incubated for 24 h at 37°C.

## *2.3. Adenoviral transduction and apoptosis assay*

Replicant-defective adenoviral vectors pAd-LacZ, pAd-T34A and pAd-D53A were generated as described previously [5]. Subconfluent cultures of A549 cells were incubated with pAd vectors at MOI 50 and the virus was allowed to adhere for 1 h at

37°C. Then medium was added and the incubation was continued under the same conditions for an additional 24 h. For the detection of apoptosis, cells were collected at indicated times from irradiation. The pellet was washed twice with PBS(-) and fixed with 1% glutaraldehyde/PBS(-) solution. The fixed cells were washed and resuspended in 20 µl of PBS(-) including 40µg/ml propidium iodide (PI) for 15 min in the dark to assess apoptotic cells. At least 200 cells were scored using an Olympus BX50 microscope (Tokyo, Japan) with reflected-light fluorescence to count cells with chromatin fragmentation and condensation as apoptotic ones.

#### *2.4. SDS-PAGE and Western blotting*

The collected cells were washed with PBS(-) and resuspended in 50 µl of lysis buffer (20 mM HEPES [pH 7.4], 2 mM EGTA, 50 mM glycerophosphate, 1% Triton X-100, 10% glycerol, 1 mM PMSF, 10 µg/ml leupeptin, 10 µg/ml aprotinin and 10 µg/ml pepstatin) and kept on ice for 30 min. After centrifugation at 15,000 rpm for 15 min at 4°C, a threefold volume of Laemmli's sample buffer (0.625 M Tris-HCl [pH6.8], 10% β-mercaptoethanol, 20% SDS, 20% glycerol, 0.004% bromophenol blue) was added to the supernatant, which was then boiled for 3 min. Proteins were separated by SDS-PAGE and transferred onto nitrocellulose membranes (ADVANTEC Toyo, Tokyo, Japan). The membranes were probed with anti-Bcl-2, anti- Bcl<sub>X<sub>L</sub></sub>, anti-Bax, anti-cleaved caspase-3 or anti-actin in TBST buffer (10 mM Tris-HCl, 0.1 M NaCl, 0.1% Tween-20, pH 7.4) containing 5% nonfat skim milk overnight at 4°C. These antibodies were detected by a method using HRP-conjugated anti-rabbit or anti-goat IgG antibodies with Perkin Elmer Western Lighting<sup>TM</sup>, Chemiluminescence Reagent Plus (Perkin Elmer Boston, MA). All western blots shown are representative of at least

two independent experiments.

### *2.5. Assays of the release of cytochrome c from mitochondria*

The cytosol of cells was prepared by a modification of the method of Bossy-Wetzol *et al.* (1997) [18]. Briefly, the cell pellet was resuspended in 300  $\mu$ l of extraction buffer, containing 250 mM sucrose, 20 mM HEPES-KOH (pH 7.4), 10 mM KCl, 1.5 mM MgCl<sub>2</sub>, 1 mM EGTA, 1 mM dithiothreitol (DTT) and 1 mM PMSF. After 1 h incubation on ice, cells were disrupted with a homogenizer and centrifuged at 1,000 g for 10 min at 4°C to remove nuclei and unbroken cells. The supernatant was further centrifuged at 26,000 g for 30 min at 4°C to separate mitochondria. The cytochrome *c* in the cytosol was detected using SDS-PAGE and western blotting as described above.

### *2.6. Electron microscopic analysis*

Cells were fixed with 3% glutaraldehyde in 0.1 M cacodylate buffer (pH 7.3) at 4°C for 4 h. After being postfixated with 2% osmium tetroxide at 4°C for 2 h, samples were dehydrated and embedded in epoxy resin. Then ultrathin sections (80 nm) were stained with uranyl acetate and lead citrate and subjected to electron microscopic observation.

### *2.7. Flow-cytometric measurement of mitochondrial membrane potential ( $\Delta\psi_m$ ) by DiOC<sub>6</sub>(3)*

To measure the mitochondrial membrane potential ( $\Delta\psi_m$ ), cells were resuspended in PBS(-) containing 10 nM 3,3'-dihexyloxyacarbocyanine iodide, DiOC<sub>6</sub>(3), and incubated for 20 min at 37°C. Then the cells were washed with PBS(-)

and resuspended in PBS(-). These cells were analyzed using an EPICS ALTRA flow cytometer (Beckman Coulter, Inc., Fullerton, CA). Two similar experiments are repeated and representative flow cytometric profiles are demonstrated.

### *2.8. Measurement of ROS production*

The fluorescent probe, 2',7'-dichlorofluorescein diacetate (DCFDA), was used for the assessment of intracellular ROS. Cells were loaded for 30 min at 37°C with 10 mM DCFDA in PBS(-). Unincorporated DCFDA was removed by two washes with PBS(-). Each sample was resuspended in PBS(-) and analyzed by flow cytometry as described above. For the detection of mitochondrial ROS, we used MitoAR, a novel fluorescent probe for selective detection of ROS in mitochondria. The MitoAR was kindly provided by Prof. T. Nagano (Graduate School of Pharmaceutical Sciences, Tokyo University) [16]. After the cells were irradiated and incubated for 6 h, they were loaded with 1  $\mu$ M MitoAR and incubated for 30 min at 37°C. Then they were observed using an Olympus IX71 microscope with reflected-light fluorescence. The fluorescence images were captured by means of a SenSys KAF1400 CCD camera (Photometrics Inc., Tucson, AZ) controlled by IPLab imaging software (Scanalytics Inc., Fairfax, VA). The photographs shown are representative of at least three times.

### *2.9. ESR spectroscopy*

Mitochondria of the cells with or without irradiation were isolated using a Mitochondria Isolation Kit (Pierce Biotechnology, Inc., Rockford, IL) and mixed with 5 mM respiratory substrates (succinate, glutamate and malate), 0.5 mM NADH, 0.2% digitonin and 10 mM CYPMPO. Then 0.2% digitonin was added to the reaction mixture

for permeation of NADH into the mitochondrial membrane [19]. The concentration of proteins in the final reaction mixture was 250  $\mu\text{g/ml}$  as evaluated according to the method described by Bradford *et al.* (Bio-Rad Laboratories, Hercules, CA) [20]. The reaction mixture was immediately transferred to a quartz flat cell (RST-DVT05; 50 mm  $\times$  4.7 mm  $\times$  0.3 mm, Radical Research) with a using a temperature controller (ES-DVT4, JEOL). The ESR spectra were recorded by using a JEOL-RE X-band spectrometer (JEOL) with a cylindrical TE011 mode cavity (JEOL). All ESR spectra were obtained at 37°C under the following conditions: 10 mW incident microwave power, 100 kHz modulation frequency, 0.1 mT field modulation amplitude and 15 mT scan range. Analysis of the hyperfine splitting constants (Hfsc) and spectral computer simulation were performed using a Win-Rad Radical Analyzer System (Radical Research). All ESR spectra shown are representative of at least three independent experiments.

### **3. Results**

#### *3.1. Radiation-induced cytochrome c release and caspase activation are inhibited by N-acetyl-L-cystein (NAC)*

In our previous study, it was demonstrated that apoptosis was enhanced by adenovirus-mediated overexpression of Survivin mutants when NIH3T3, HeLa and A549 cells were irradiated with X rays and incubated for 48 h [5]. First, to clarify the relationship between cytochrome *c* release from mitochondria and radiation-induced apoptosis in the cells which lacked Survivin function, the time course of the radiation-induced apoptosis in the cells overexpressing Survivin mutants was compared with that of cytochrome *c* release from mitochondria. The time course of apoptosis induced by combination of Survivin mutants and radiation is shown in Fig. 1a. When

T34A (a phosphorylation-defect mutant; closed square in Fig. 1a) and D53A (defective in binding activity with Smac/DIABLO; open triangle in Fig. 1a) were overexpressed in A549 cells, apoptotic cells with morphological changes such as chromatin fragmentation and condensation were significantly increased at 24 h after irradiation, whereas, the cells that overexpressed LacZ (closed circle in Fig. 1a) did not exhibit apoptosis. On the other hand, cytochrome *c* was released from mitochondria to cytosol already at 24 h after irradiation (Fig. 1b). Next, to clarify the presence of redox regulation in radiation-induced cytochrome *c* release from mitochondria, the effects of post-irradiation-treatments with various antioxidants and a flavoprotein inhibitor were examined. When three antioxidants, NAC, Trolox and S-PBN and one flavoprotein inhibitor, DPI, were added to the medium just after irradiation and incubated for 24 h, these compounds completely inhibited the radiation-induced cytochrome *c* release from mitochondria to cytosol, as shown in Fig 1c. Moreover, post-irradiation-treatment with NAC inhibited the radiation-induced apoptosis in A549 cells overexpressing Survivin dominant negative mutants, pAd-T34A and pAd-D53A (Fig 1d). As shown in Fig. 1e, the cleaved fragments of caspase-3 (p19 and p17; active form of caspase-3) were induced in irradiated cells overexpressing Survivin mutants. However, these inductions of cleaved caspase-3 were inhibited by post-irradiation-treatment with NAC.

### *3.2. Expression of Bcl-2 family is not influenced by NAC.*

Since cytochrome *c* release from mitochondria is generally believed to be regulated by the balance between the proapoptotic Bcl-2 family and antiapoptotic Bcl-2 family [21]. The expression of Bcl-2, Bcl-X<sub>L</sub> and Bax was evaluated by western blotting. As shown in Fig. 2a, the expression of the antiapoptotic Bcl-2 family members Bcl-2

and Bcl-X<sub>L</sub> was slightly increased at 12, 24 and 36 h after irradiation. In contrast, that of the proapoptotic Bcl-2 family member Bax was remarkably increased at 6 and 12 h after irradiation. Since the cytochrome *c* release occurred at 24 h after irradiation and the ratios of Bax to Bcl-2 (Bax/Bcl-2) at 6 and 12 h after irradiation were high, the effect of the post-irradiation treatment with NAC on the expression of the Bcl-2 family was examined to clarify the relationship between Bax expression and redox regulation. As shown in Fig. 2b, treatment with NAC did not affect either radiation-induced expression of Bax or Bcl-2 and Bcl-X<sub>L</sub>.

### *3.3. X irradiation enhances late intracellular ROS from mitochondria with increased mitochondrial membrane potential ( $\Delta\psi_m$ )*

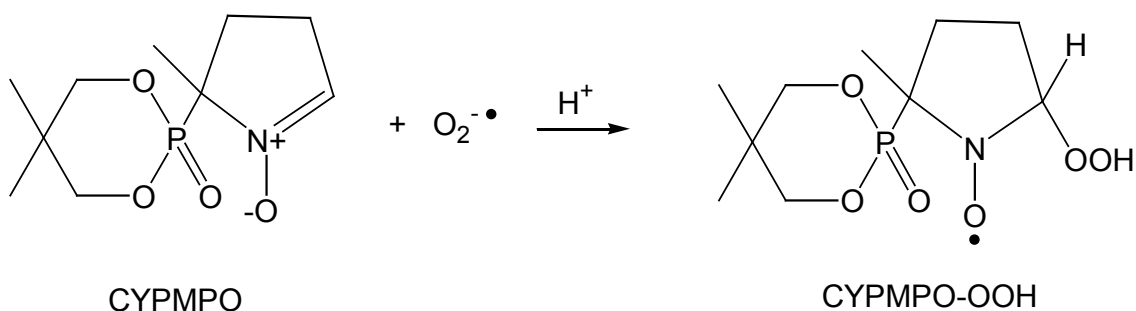
To analyze the effect of irradiation on mitochondria, morphological analysis and measurement of mitochondrial membrane potential ( $\Delta\psi_m$ ) were performed. As shown in Fig. 3, the mitochondrial shape and structure were not changed at 12 and 24 h after irradiation, although cytochrome *c* release from mitochondria had already occurred 24 h after irradiation. The uptake of the  $\Delta\psi_m$ -sensitive reagent DiOC<sub>6</sub>(3) into mitochondria is dependent on the  $\Delta\psi_m$ . As shown in Fig. 4a, the cell population having stronger fluorescence increased from 4.8% to 28.6% and 35.0% when cells were incubated for 12 h and 24 h after irradiation with 10 Gy X rays, respectively, suggesting that the  $\Delta\psi_m$  was time-dependently elevated by X irradiation (Fig. 4a). This increase of the  $\Delta\psi_m$  was sustained until 48 h. Since radiation-induced cytochrome *c* release was suggested to be regulated by ROS (Fig. 2a), we next tried to measure the late production of intracellular ROS in irradiated A549 cells. For this purpose, we employed two intracellular ROS indicators. One was the classical

ROS-sensitive fluorescence probe 2,7-dichlorodihydrofluorescein diacetate (DCFDA). In left panel of Fig. 4b, flow cytometric analysis using this probe reveals that the ROS production started to increase at 6 h after irradiation and reached the maximum, about three-fold in comparison with that of the untreated control (the right panel of Fig 4b), at 12 h after irradiation. To determine the organelle responsible for the radiation-induced ROS production, we used another fluorescence probe, MitoAR (Fig. 4c), which is selectively localized in mitochondria and reacts with ROS [16]. If unirradiated cells were loaded with MitoAR and incubated for 30 min at 37°C, weak fluorescence was observed (left panel of Fig. 4d). At 6 h after irradiation, cells were loaded with MitoAR and incubated for 30 min at 37°C, and then we observed several cells with strong fluorescence as shown in the middle panel of Fig. 4d. This cell population with strong fluorescence disappeared in the presence of NAC (right panel of Fig. 4d).

#### *3.4. X-irradiation enhances the ability of NADH/succinate-dependent $O_2^-$ production from mitochondria isolated from A549 cells*

Since MitoAR clearly demonstrated that mitochondrial ROS was increased at 6 h after irradiation (Fig. 4d), mitochondria seem to be candidate organelles for the increase in late intracellular ROS after irradiation. Therefore, the production ability of  $O_2^-$  in mitochondria was studied by the ESR/spin-trapping technique in a cell-free system. The mitochondrial fraction isolated from A549 cells without X irradiation was incubated in the presence of 5 mM respiratory substrates (succinate, glutamate and malate), 0.5 mM NADH, 0.2% digitonin and 10 mM CYPMPO. It was reported that 0.2% digitonin punctured mitochondrial membrane to allow NADH to penetrate inside

of the mitochondria [19]. After incubation in the reaction mixture for 25 min at 37°C, the ESR spectrum in (I) shown in Fig. 5 was observed. This spectrum consists of two isomers (isomer A; Hfsc for  $A_N$ ,  $A_H$  and  $A_P$  are 1.34, 1.19 and 5.15 mT, isomer B; Hfsc for  $A_N$ ,  $A_H$  and  $A_P$  are 1.35, 1.07 and 4.95 mT) and was reproduced with a computer spectrum simulation (data not shown). These Hfsc parameters were quite similar to those of the ESR spectrum (VI) produced by the hypoxanthine (HX)/xanthine oxidase (XOD) system used as a well-established  $O_2^{\cdot-}$  source and those of CYPMPO-OOH spin adducts as reported previously [17]. From these facts, spectrum (I) was assigned to the CYPMPO-OOH spin adduct formed by the reaction of  $O_2^{\cdot-}$  with CYPMPO as the following equation.



Typical time course in Fig. 5b show that the intensity of ESR signals due to CYPMPO-OOH was time-dependently increased and reached the maximum at 25 min. Moreover, the signal intensity of this ESR spectrum obtained after incubation for 25 min was considerably reduced in the absence of either digitonin (II) or succinate (III). The absence of NADH (IV) and the addition of SOD (V) completely abolished the ESR signals. Finally, NADH/succinate-dependent  $O_2^{\cdot-}$  in mitochondria isolated from unirradiated A549 cells was compared with that from irradiated cells (Fig. 5c). The results presented in Fig.5d showed that the ESR signal intensity of CYPMPO-OOH in mitochondria isolated from irradiated cells was significantly increased, about 1.6-fold,

in comparison with that from unirradiated cells.

## **Discussion**

It is generally considered that genotoxic reagents promote mitochondria-mediated apoptotic signaling such as cytochrome *c* release from mitochondria, followed by activation of caspase-9 and -3 through formation of a complex with Apaf-1 and the caspase-activated deoxyribonuclease (DNase)(CAD) pathway [22,23]. However, in several radioresistant solid tumor cells, the constitutive anti-apoptotic proteins seem to inhibit this apoptotic signaling because radiation sometimes induces cytochrome *c* release from mitochondria without induction of apoptosis, as shown in our previous study [5] and Fig. 1b. In the case of A549 cells, constitutive Survivin was found to suppress the downstream signaling of mitochondria and dysfunction of constitutive Survivin by transduction of pAd-T34A, and pAd-D53A facilitated this apoptotic downstream signaling [5]. Thus, cytochrome *c* release from mitochondria is an essential event for radiation-induced apoptotic signaling in not only hematopoietic cell lines but also solid tumor cell lines that lack intrinsic function of Survivin; however, the mechanism for radiation-induced cytochrome *c* release is still unclear.

As cytochrome *c* release from mitochondria is widely believed to be regulated by the balance between proapoptotic and antiapoptotic Bcl-2 family members [21], the expression of Bcl-2, Bcl-X<sub>L</sub> and Bax was evaluated by western blotting. As can be seen in Fig. 2a, X irradiation increased the expression of proapoptotic Bax prior to cytochrome *c* release from mitochondria in A549 cells, suggesting that enhancement of the expression of proapoptotic Bax relative to antiapoptotic Bcl-2 and Bcl-X<sub>L</sub> triggered

mitochondrial dysfunction to lead to cytochrome *c* release from the mitochondria. However, the mitochondrial membrane potential ( $\Delta\psi_m$ ) was increased without morphological changes such as swelling (Fig. 3) and sustained at least for 48 h after irradiation (Fig. 4a). Interestingly, radiation-induced cytochrome *c* release was completely abolished by post-irradiation-treatments with a variety of antioxidants and a flavoprotein inhibitor (Fig. 1c), although the chemical reaction of biomolecules with primary ROS produced by water radiolysis is believed to finish within  $\sim 10^{-9}$  seconds. These results suggested the presence of late production of ROS tightly associated with cytochrome *c* release, followed by apoptosis. The radiation-induced expression of Bax was not affected by post-irradiation treatment with NAC (Fig. 2b), suggesting that radiation-induced expression of the Bcl-2 family was independent of redox regulation and the proapoptotic protein Bax regulated ROS production to lead cytochrome *c* release from mitochondria. In addition, flow cytometric analysis using DCFDA showed late intracellular ROS at 6, 12 and 24 h after irradiation (Fig. 4b). In programmed neuronal death induced by deprivation of nerve growth factor (NGF), Kirkland *et al.* reported that Bax translocated from cytoplasm to mitochondria and induced the release of cytochrome *c* through an increase of intracellular ROS [24]. Taken together, these findings suggest that radiation-induced overexpression of Bax initiates an increase of ROS to induce cytochrome *c* release from mitochondria.

Several cellular sources can generate ROS: peroxisomes, plasma membrane proteins, such as NADPH oxidase, cytosolic enzymatic reactions and mitochondria. Recently, in leukemia Jurkat T cells, it was reported that  $\gamma$ -irradiation-induced cytochrome *c* release from mitochondria and activation of caspases were inhibited by the mitochondrial complex I inhibitor rotenone [14]. Lee *et al.* showed that increased

expression of mitochondrial NADP<sup>+</sup>-dependent isocitrate dehydrogenase (IDPms), which is a key enzyme in the cellular defense against oxidative damage, suppressed  $\gamma$ -irradiation-induced ROS generation and apoptotic cell death [25]. In contrast to these mitochondria-derived ROS, Tateishi *et al.* showed that  $\gamma$  irradiation induced the expression of NOX1, categorized in the NADPH oxidase (NOX) family, and the intracellular ROS level was increased [26]. They also demonstrated that siRNA against NOX1 reduced the intracellular ROS level and radiation-induced apoptotic cell death in immortalized salivary gland acinar cells [26]. Thus, the source of late intracellular ROS in tumor cells exposed to ionizing radiation and genotoxic reagents is still controversial. In this experiment, to obtain direct evidence that mitochondria are candidates for the organelle source of ROS in tumor cells exposed to X irradiation, we employed the novel fluorescence ROS indicator MitoAR to clarify the localization of ROS production by fluorescent microscopy in living cells and the novel spin-trapping reagent CYPMPO to identify radical species by ESR spectroscopy in a cell-free system. As shown in Fig. 4d, the accumulation of ROS in mitochondria was demonstrated in the cells at 6 h after irradiation. By using CYPMPO which has advantages for the stability of spin adducts and detection sensitivity as a spin-trapping reagent, we succeeded in detection of NADH/succinate-dependent O<sub>2</sub><sup>-</sup> production of mitochondria treated with 0.2% digitonin, as shown in Fig. 5a. Moreover, the enhancement of NADH/succinate-dependent O<sub>2</sub><sup>-</sup> production was observed in mitochondria isolated from A549 cells incubated for 6 h after irradiation (Fig. 4c). However, the mechanism for the radiation-induced enhancement of O<sub>2</sub><sup>-</sup> production in mitochondria remains unclear. Since we observed that NADH/succinate-dependent O<sub>2</sub><sup>-</sup> in isolated mitochondria was enhanced by X irradiation and mitochondrial membrane potential was

sustained at high level after irradiation, there is a possibility that  $O_2^-$  leaking from the respiratory chain including complexes I~III, which are important in the electron transport system from succinate and NADH, may be enhanced by X irradiation. Further experiments and analysis of the status of complexes I~III will be necessary to clarify how ROS accumulation in mitochondria occurs after X irradiation.

From these results, we concluded that ionizing radiation enhanced  $O_2^-$  production from mitochondria to trigger cytochrome *c* release in A549 cells, as shown in the summary in Fig. 6. This is the first direct evidence that mitochondria are source of late intracellular ROS in tumor cells exposed to genotoxic stimuli. The data obtained from our experiments may help us to propose new therapeutic targets such as intrinsic enzymes and substances against oxidative stress, e.g., MnSOD, glutathione and thioredoxin reductase.

### **Conflict of Interest**

All of the authors declare no conflict of interests with this work.

### **Acknowledgements**

The authors are grateful to Prof. T. Nagano, Dr. Y. Urano and Dr. Y. Koide (Graduate School of Pharmaceutical Sciences, Tokyo University) for MitoAR. This work was supported, in part, by Grants-in-Aid for Basic Scientific Research from the Ministry of Education, Culture, Sports, Science and Technology, Japan (No.17380178, No.18658118 and No. 19380172 [O.I.]), by the JSPS Research Fellowship for Young Scientists [H.Y.] and JSPS Core-to-Core Program [A.O.]. The authors thank Dr. T. Asanuma and Dr. K. Waki for their technical assistance.

## References

- [1] D.R. Green, J.C. Reed, Mitochondria and apoptosis, *Science* 281 (1998) 1309-1312.
- [2] C. Du, M. Fang, Y. Li, L. Li, X. Wang, Smac, a mitochondrial protein that promotes cytochrome *c*-dependent caspase activation by eliminating IAP inhibition, *Cell* 102(2000) 33-42.
- [3] D. R. Aldridge, I. R. Radford, Explaining differences in sensitivity to killing by ionizing radiation between human lymphoid cell lines, *Cancer Res.* 58 (1998) 2817–2824.
- [4] K. Takahashi, O. Inanami, M. Hayashi, M. Kuwabara, Protein synthesis-dependent apoptotic signalling pathway in X-irradiated MOLT-4 human leukaemia cell line, *Int. J. Radiat. Biol.* 78 (2002) 115-124.
- [5] A. Ogura, Y. Watanabe, D. Iizuka, H. Yasui, M. Amitani, S. Kobayashi, M. Kuwabara, O. Inanami, Radiation-induced apoptosis of tumor cells is facilitated by inhibition of the interaction between Survivin and Smac/DIABLO, *Cancer Lett.* 259 (2008) 71-81.
- [6] P.A. Riley, Free radicals in biology: oxidative stress and the effects of ionizing radiation, *Int. J. Radiat. Biol.* 65 (1994) 27-33.
- [7] S.S. Wallace, Enzymatic processing of radiation-induced free radical damage in DNA, *Radiat. Res.* 150 (1998) s60-79.
- [8] H. Tominaga, S. Kodama, N. Matsuda, K. W. Suzuki, M. Watanabe, Involvement of reactive oxygen species (ROS) in the induction of genetic instability by radiation, *J. Radiat. Res.* 45 (2004) 181-188.
- [9] T. Tsuzuki, Y. Nakatsu, Y. Nakabeppu, Significance of error-avoiding mechanisms

- for oxidative DNA damage in carcinogenesis, *Cancer Sci.* 98 (2007) 465-470.
- [10] T. Hamasu, O. Inanami, T. Asanuma, M. Kuwabara, Enhanced induction of apoptosis by combined treatment of human carcinoma cells with X rays and death receptor agonists, *J. Radiat. Res.* 46 (2005) 103-110.
- [11] T. Hamasu, O. Inanami, M. Tsujitani, K. Yokoyama, E. Takahashi, I. Kashiwakura, M. Kuwabara, Post-irradiation hypoxic incubation of X-irradiated MOLT-4 cells reduces apoptotic cell death by changing the intracellular redox state and modulating SAPK/JNK pathways, *Apoptosis* 10 (2005) 557-567.
- [12] O. Inanami, K. Takahashi, M. Kuwabara, Attenuation of caspase-3-dependent apoptosis by Trolox post-treatment of X-irradiated MOLT-4 cells, *Int. J. Radiat. Biol.* 75 (1999) 155-163.
- [13] Q. Chen, Y.C. Chai, S. Mazumder, C. Jiang, R.M. Macklis, G.M. Chisolm, A. Almasan, The late increase in intracellular free radical oxygen species during apoptosis is associated with cytochrome *c* release, caspase activation, and mitochondrial dysfunction, *Cell Death Differ.* 10 (2003) 323-334.
- [14] Y.J. Lee, D.H. Lee, C.K. Cho, H.Y. Chung, S. Bae, G.J. Jhon, J.W. Soh, D.I. Jeoung, S.J. Lee, Y.S. Lee, HSP25 inhibits radiation-induced apoptosis through reduction of PKC $\delta$ -mediated ROS production, *Oncogene* 24 (2005) 3715-3725.
- [15] Y. Ni, X.G. Gong, M. Lu, H.M. Chen, Y. Wang, Mitochondrial ROS burst as an early sign in sarsasapogenin-induced apoptosis in HepG2 cells, *Cell Biol. Int.* 32 (2008) 337-343.
- [16] Y. Koide, Y. Urano, S. Kenmoku, H. Kojima, T. Nagano, Design and synthesis of fluorescent probes for selective detection of highly reactive oxygen species in mitochondria of living cells, *J. Am. Chem. Soc.* 129 (2007) 10324-10325.

- [17] M. Kamibayashi, S. Oowada, H. Kameda, T. Okada, O. Inanami, S. Ohta, T. Ozawa, K. Makino, Y. Kotake, Synthesis and characterization of a practically better DEPMPO-type spin trap, 5-(2,2-dimethyl-1,3-propoxy cyclophosphoryl)-5-methyl-1-pyrroline N-oxide (CYPMPO), Free Radic. Res. 40 (2006) 1166-1172.
- [18] E. Bossy-Wetzol, D.R. Green. Assays for cytochrome c release from mitochondria during apoptosis, Methods Enzymol. 322 (2000) 235-242.
- [19] D. Han, E. Williams, E. Cadenas, Mitochondrial respiratory chain-dependent generation of superoxide anion and its release into the intermembrane space, Biochem. J. 353 (2001) 411-416.
- [20] M.M. Bradford, A rapid and sensitive method for the quantitation of microgram quantities of protein utilizing the principle of protein-dye binding, Anal. Biochem. 72 (1976) 248-254.
- [21] S. Cory, J.M. Adams, The Bcl2 family: regulators of the cellular life-or-death switch, Nat. Rev. Cancer 2 (2002) 647-656.
- [22] N. Taneja, R. Tjalkens, M.A. Philbert, A. Rehemtulla, Irradiation of mitochondria initiates apoptosis in a cell free system, Oncogene 20 (2001) 167-177.
- [23] K.M. Hajra, J.R. Liu, Apoptosome dysfunction in human cancer, Apoptosis 9 (2004) 691-704.
- [24] R.A. Kirkland, J.A. Windelborn, J.M. Kasprzak, J.L. Franklin, A Bax-induced pro-oxidant state is critical for cytochrome *c* release during programmed neuronal death, J. Neurosci. 22 (2002) 6480-6490.
- [25] J.H. Lee, S.Y. Kim, I.S. Kil., J.W. Park, Regulation of ionizing radiation-induced apoptosis by mitochondrial NADP<sup>+</sup>-dependent isocitrate dehydrogenase, J. Biol.

Chem. 282 (2007) 13385-13394.

[26] Y. Tateishi, E. Sasabe, E. Ueta, T. Yamamoto, Ionizing irradiation induces apoptotic damage of salivary gland acinar cells via NADPH oxidase 1-dependent superoxide generation, *Biochem. Biophys. Res. Commun.* 366 (2008) 301-307.

### Legends to figures

**Fig. 1.** Effects of antioxidants on apoptosis and cytochrome *c* release in A549 cells exposed to X rays. (a) At 24 h after transduction with pAd-LacZ, pAd-T34A or pAd-D53A, A549 cells were irradiated with 10 Gy of X rays and then further incubated for 3, 6, 12, 24, 36 and 48 h. After PI staining, at least 200 cells were scored using fluorescence microscopy to count cells with chromatin fragmentation and condensation as apoptotic ones. Data are expressed as means  $\pm$  SE for three experiments. \*\*Significantly different from pAd-LacZ in each incubation time ( $p < 0.01$ , Student's *t*-test). (b) At 6, 12, 24 and 36 h after X irradiation, cytosolic cytochrome *c* was examined by western blotting. (c) The effects of various antioxidants on radiation-induced cytochrome *c* release. After X irradiation, cells were incubated for 24 h in medium containing 20 mM NAC, 10 mM Trolox, 15 mM S-PBN and 70  $\mu$ M DPI as described in Materials and Methods. (d) Effects of 20 mM NAC on radiation-induced apoptosis enhanced by Survivin mutants. After irradiation, cells overexpressing Survivin mutants were incubated for 48 h with 20 mM NAC. Apoptotic cells were evaluated using a protocol similar to that described above. Data are expressed as means  $\pm$  SE for three experiments. \*\*Significantly different from absence of NAC ( $p < 0.01$ , Student's *t*-test). (e) At 48 h after each treatment, the cleaved caspase-3 (p19 and p17, active form of caspase-3) was evaluated by western blotting.

**Fig. 2.** Effects of post-irradiation-treatment with NAC on expression of Bcl-2 family members. (a) After incubation of X-irradiated A549 cells for 6, 12, 24, 36 and 48 h, the expression of Bcl-2, Bcl-X<sub>L</sub>, Bax and actin was examined by western blotting. The ratio of Bax to Bcl-2 (Bax/Bcl-2) is shown at the bottom. (b) After irradiation, 20 mM NAC was added to the medium and cells were incubated for 12 h. Then the expression of the Bcl-2 family members as analyzed by western blotting using a protocol similar to that described above. Typical blotting patterns were shown in (a) and (b).

**Fig. 3.** Electron-microscopic images of A549 cells. (a) unirradiated control, (b) 12 h after X irradiation and (c) 24 h after X irradiation. Black bar indicates 200 nm.

**Fig. 4.** Measurements of the production of intracellular ROS in A549 cells with or without irradiation. (a) The flow cytometric profiles of the cells stained for 15 min at 37°C with a mitochondrial-membrane-potential ( $\Delta\psi_m$ )-sensitive reagent, DiOC<sub>6</sub>(3), when A549 cells were incubated for 12, 24 and 48 h after exposure to 10 Gy of X rays. (b) Left pane: typical flow cytometric profiles of cells stained for 30 min at 37°C with the intracellular ROS-sensitive reagent, 2,7-dichlorodihydrofluorescein diacetate (DCFDA), when A549 cells were incubated for 0 and 12 h after exposure to 10 Gy of X rays. Right panel: The time course of relative intracellular ROS evaluated by flow cytometric analysis using DCFDA. Each column and vertical bar show mean  $\pm$  SE for three experiments. \*Significantly different from 0 h after irradiation ( $p < 0.05$ , Student's *t*-test). (c) The chemical structure of MitoAR. (d) After cells were irradiated and incubated for 6 h with or without NAC, cells were incubated for 30 min at 37°C in the

presence of 1  $\mu\text{M}$  MitoAR. Typical photographs of difference interference contrast (DIC) and fluorescence microscopy (MitoAR) are shown in upper and lower panels, respectively.

**Fig. 5.** Detection of NADH/succinate-dependent  $\text{O}_2^{\cdot-}$  production in isolated mitochondria and effect of X irradiation on this NADH/succinate-dependent  $\text{O}_2^{\cdot-}$  production. (a) ESR spectra produced using the spin-trap CYPMPO. ESR spectra (I) and (II) were obtained when isolated mitochondria were incubated for 25 min at  $37^\circ\text{C}$  in the presence of 10 mM CYPMPO, 5 mM respiratory substrates (succinate, glutamate and malate) and 0.5 mM NADH with and without 0.2% digitonin, respectively. ESR spectrum (III) and (IV) were obtained when succinate or NADH was deleted from the conditions used to obtain spectrum (I). ESR spectrum (V) was obtained when 20 U/ml SOD was added to the reaction mixture used to obtain spectrum (I). ESR spectrum (VI) was obtained when aqueous solution containing 250  $\mu\text{M}$  hypoxanthine, 25 mU/ml hypoxanthine oxidase, 0.1 mM DATAPAC and 10 mM CYPMPO was incubated for 5 min. (b) Typical time course of ESR signal intensities (h indicated in central component of ESR spectrum) obtained in conditions (I)~(IV). (c) Upper panel: ESR spectrum was obtained when mitochondria isolated from unirradiated cells were incubated for 25 min at  $37^\circ\text{C}$  in the presence of 10 mM CYPMPO, 5 mM respiratory substrates (succinate, glutamate and malate), 0.5 mM NADH and 0.2% digitonin for 25 min at  $37^\circ\text{C}$ . Lower panel: ESR spectrum was obtained from isolated mitochondria of X-irradiated cells. ESR signal intensities (arbitrary units) obtained from three independent experiments were summarized as shown in (e). Data are expressed as means  $\pm$  SE for three experiments. \*Significantly different from unirradiated group ( $p < 0.05$ , Student's *t*-test).

**Fig. 6.** Summary of redox regulation for radiation-induced cytochrome *c* release suggested by data shown in the previous figures. fp; flavoprotein

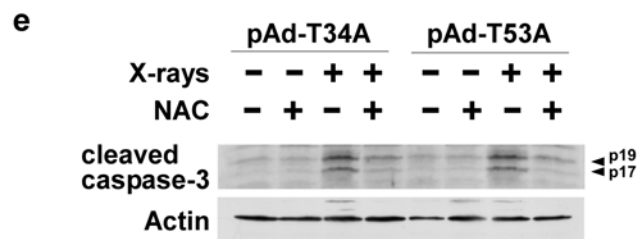
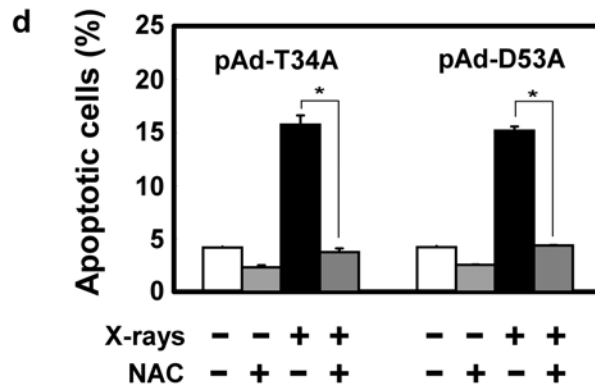
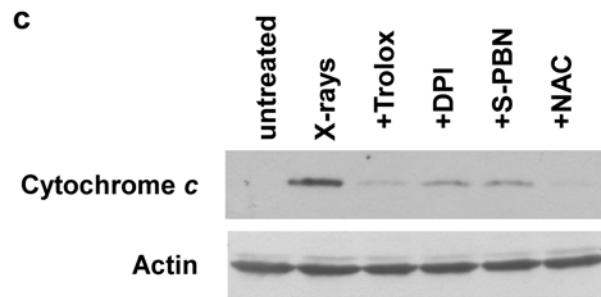
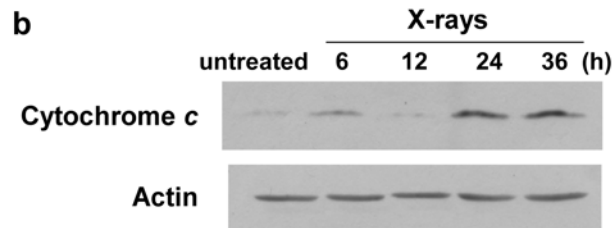
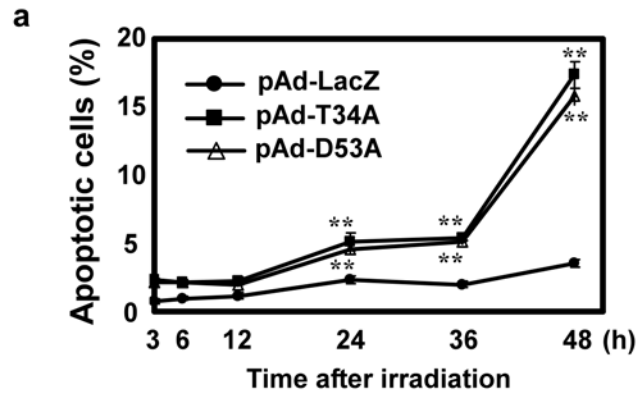
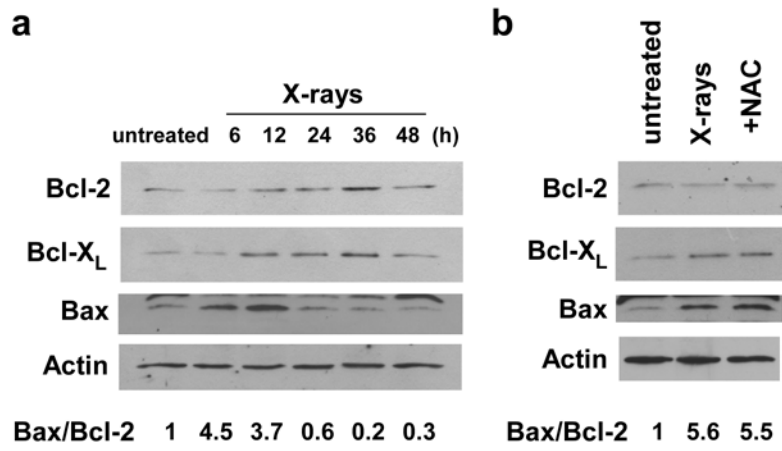
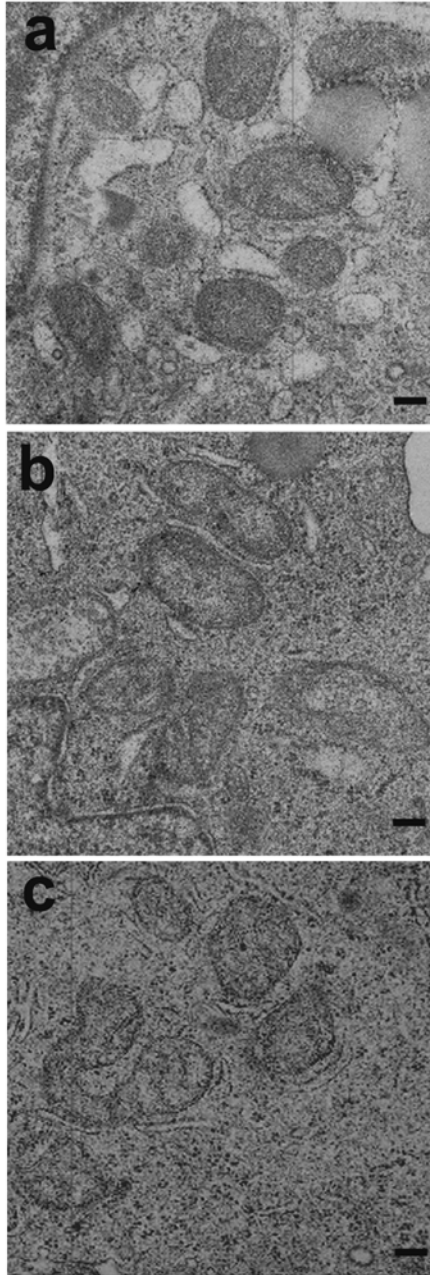


Fig. 1 Ogura *et al.*



**Fig. 2** Ogura *et al.*



**Fig. 3** Ogura *et al.*

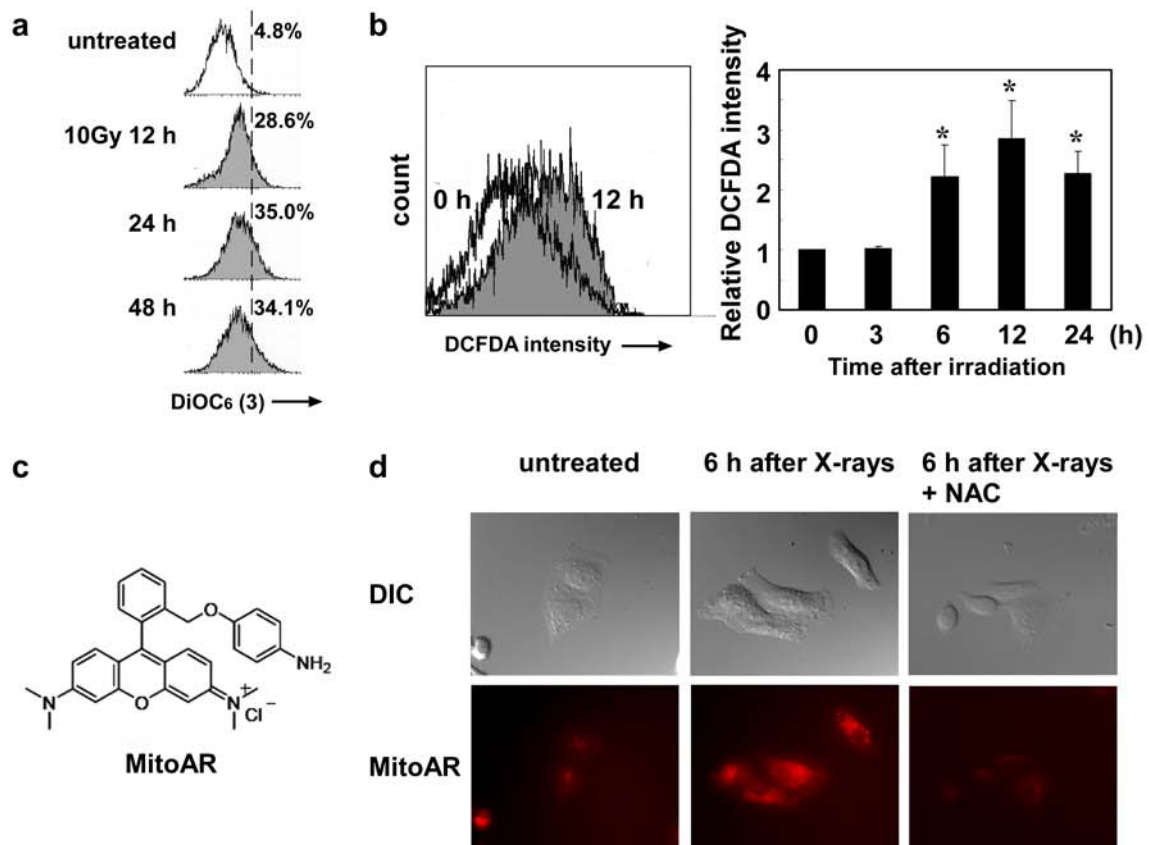


Fig. 4 Ogura *et al.*

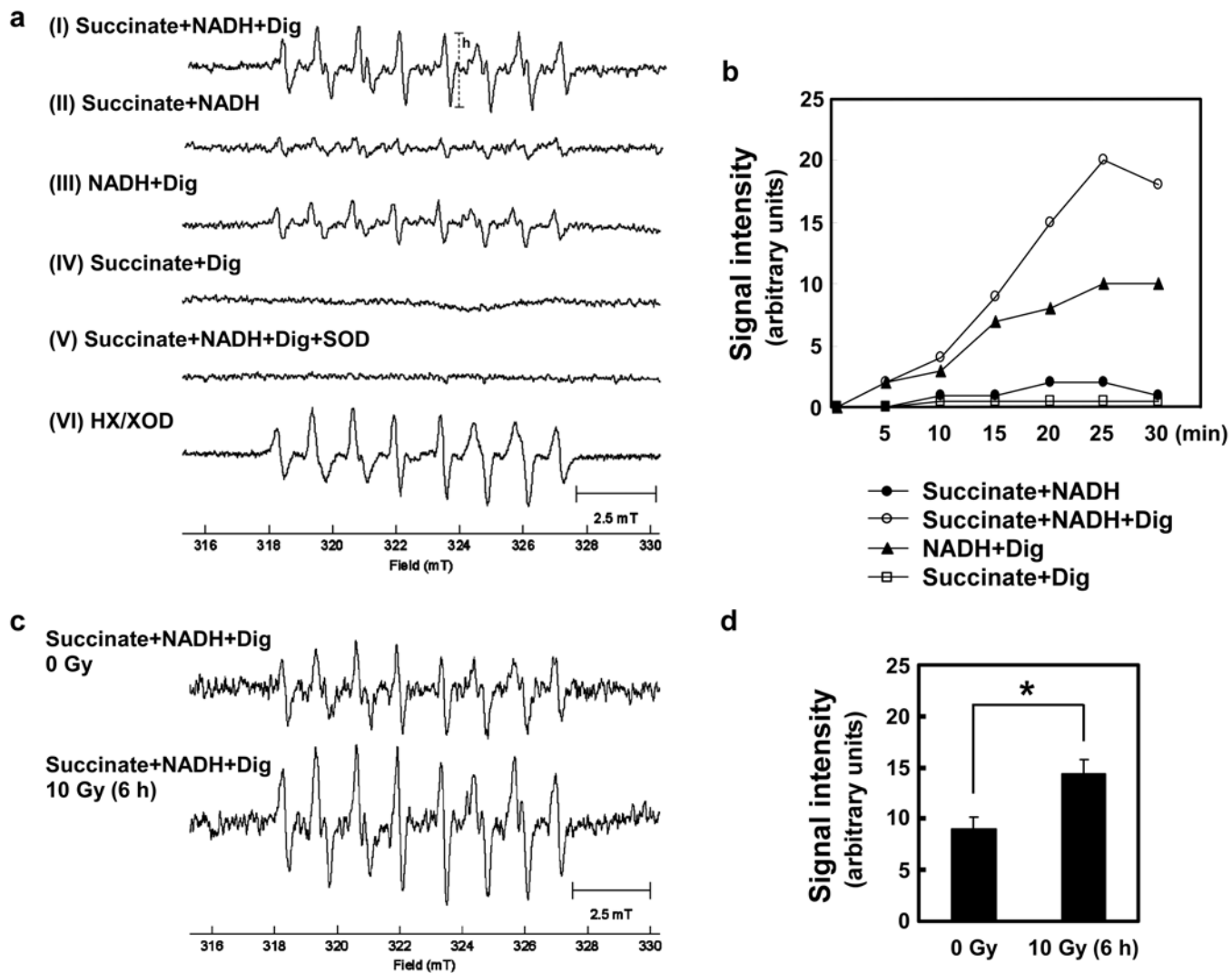


Fig. 5 Ogura *et al.*

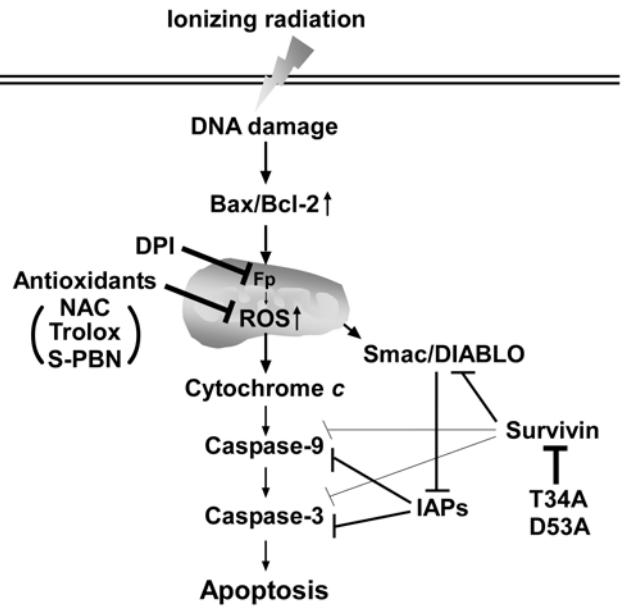


Fig. 6 Ogura *et al.*